Magnetism and crystal structure in orthorhombic Fe_2P: a theoretical and experimental study

1995 J. Phys.: Condens. Matter 7 185

(http://iopscience.iop.org/0953-8984/7/1/016)

J. Phys.: Condens. Matter 7 (1995) 185–198. Printed in the UK

Magnetism and crystal structure in orthorhombic Fe_2P: a theoretical and experimental study

L Severin†‖, L Häggström†, L Nordström‡, Y Andersson§ and B Johansson†

† Department of Physics, University of Uppsala, Box 530, S-75121 Uppsala, Sweden

‡ Forschungzentrum Jülich GmbH, Postfach 1913, D-5170 Jülich, Germany

§ Department of Chemistry, University of Uppsala, Box 531, S-75121 Uppsala, Sweden

Received 5 May 1994, in final form 15 September 1994

Abstract. A theoretical and experimental study of the electronic and magnetic structure of $Fe_2P_{1-x}Si_x$ is performed. A hexagonal–orthorhombic crystal structure transition occurs with increasing Si substitution. The latter crystal structure is extremely complex with six inequivalent Fe sites. The magnetic moments, as obtained by our electronic structure calculations, vary substantially between the different sites, from $0.7\mu_B$ to $2.6\mu_B$. The latter value is one of the largest Fe moments ever found. The estimated hyperfine fields are in fair agreement with Mössbauer data. For this compound it is found that the hyperfine field cannot be assumed to be proportional to the spin magnetic moment when the majority spin band is saturated. This is explained in terms of a hybridization mechanism between the Fe 3d and 4s states, which results in a 4s valence electron contribution that may be large and of either sign.

1. Introduction

The iron phosphide compound Fe_2P forming in the hexagonal crystal structure has attracted much experimental as well as theoretical attention due to its peculiar magnetic properties. (A recent review is given by Beckman and Lundgren [1]). Thus a first-order transition is observed with temperature with a change of crystal structure parameters as well as magnetization. Moreover the hexagonal compound exhibits a metamagnetic transition at relatively low magnetic fields suggesting two magnetic solutions to be nearly degenerate in energy. From a technological point of view Fe_2P is interesting due to its large uniaxial magnetocrystalline anisotropy, thus being a candidate for a good permanent magnet. However due to its low Curie temperature it has not found commercial use. A main stream in applied research has therefore been to try to increase the Curie temperature by certain alloying substitutions without decreasing the anisotropy. Experimentally such substitutions have shown to alter the magnetic properties significantly, e.g. a 1% substitution of Mn for Fe gives a metamagnet. Up to 15% of the P atoms may be replaced by B without changing the hexagonal crystal structure. B substitutions have been found to increase the Curie temperature to values as high as about 500 K. Substitutions by Si, however may be made to up to 30% with a maximum $T_c = 600$ K. At Si concentrations above $\sim 10\%$ a transition from the hexagonal structure to a more complicated body centred orthorhombic (BCO) structure occurs [2]. Theoretically, early attempts [3] to account for the magnetic interactions were based on the Heisenberg model. However Wohlfarth [4] and Moriya and Usami [5] presented

‖ Present address: Institut für Festkörperphysik, Technische Hochschule Darmstadt, Hochschulstrasse 6/8, D-64289 Darmstadt, Germany.

0953-8984/95/010185+14$19.50

arguments in favour of a description based upon itinerant magnetism. Experimental evidence for such a picture was then found from the very small entropy (0.02 R) of the first-order magnetic transition [6]. Later accurate first-principles calculations by Eriksson *et al* [7], based upon the local spin density approximation (LSDA), for the hexagonal structure gave magnetic moments in fair agreement with experimental data. Similar calculations were also performed by Ishida *et al* [8] for the T_2P (T = Mn, Fe, Ni) compounds. These two sets of calculations were found to be consistent with one another.

Calculations employing the LSDA have been extremely successful in accounting for the magnetic structure of weakly correlated ferromagnetic systems. Thus a lot of attention is naturally devoted to the borderline cases, where correlations may play a major role in the electronic structure. These systems are mainly the f elements, i.e. the lanthanides and the actinides, and their compounds. Very little effort, though, has been made to describe weakly correlated, but complex systems. In this respect the BCO structure is ideally suited for an investigation, since its unit cell with six different Fe atom types and three different types of P site clearly poses a challenge for theory.

Therefore, in this work we concentrate on the hexagonal–orthorhombic structural transition occurring with increasing Si substitution. In the next section we describe the crystal structures studied in this paper; the experimental results are given in section 3, while our theoretical analysis is presented in section 4. Conclusions are given in section 5.

2. Crystallographic structures of Fe_2P

The crystallographic structure of Fe_2P is hexagonal (space group $P6\ 2m$) and there are two inequivalent Fe as well as P sites. We refer to them as Fe(I), Fe(II), P(I), and P(II). In the hexagonal unit cell there are two atoms of type P(I), one of type P(II) and three atoms of both type Fe(I) and type Fe(II). At $T_c \approx 216$ K, a first-order transition occurs with a change of lattice parameters and onset of ferromagnetism. Spin polarized electronic structure calculations by Eriksson *et al* [7] revealed a magnetic ground state with moments equal to $0.96\mu_B$ for the Fe(I) site and $2.04\mu_B$ for the Fe(II) site. The total magnetic moment was calculated to be $2.94\mu_B$ due to the small moments on the P atoms coupled antiparallel to the Fe moments. These theoretical results were compared with polarized neutron scattering data (scaled to saturation): Fe(I), $1.03\mu_B$; Fe(II), $1.91\mu_B$. In general a good description of the ground state magnetic structure, hyperfine fields, and isomer shifts was obtained in that study, thus concluding that an LSDA based approach should be appropriate for this compound.

A phase diagram of $Fe_2P_{1-x}Si_x$ is shown in figure 1. Interestingly, with increasing Si substitution a structural change from hexagonal to orthorhombic is observed [2]. This sensitivity to external perturbations can be seen from for example the large contribution to the specific heat (25 mJ K^{-2}) that is experimentally observed [6]. Eriksson *et al* [7] found an almost saturated majority spin band and hence the state density for the up spin direction is much smaller than that for the down spin direction. In this respect the hexagonal Fe_2P should then be characterized as a weak itinerant ferromagnet [9], and its properties will be strongly dependent on external perturbations.

In the BCO structure, there are three different types of P atoms and six different types of Fe sites, labelled P(1), P(2), P(3), Fe(1), Fe(2), etc. There will be no risk of confusing the sites between the structures, since we always use roman numbers for the hexagonal phase and arabic numbers for the orthorhombic phase. The atomic positions and the symmetry labels of the sites in the BCO structure are given in table 1.

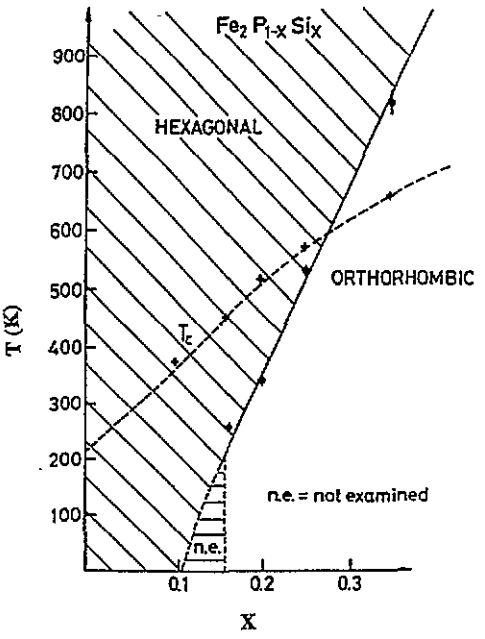

Figure 1. A phase diagram of the hexagonal–BCO phase transition as a function of temperature and increasing Si concentration (x). The Curie temperature is plotted with a dashed line and denoted T_c. (From [2].)

Table 1. Lattice parameters and atomic positions used in the calculation for the BCO crystal structure [10].

Space group	*Imm*2			
Lattice parameters	$a = 6.533$ Å	$b = 10.3632$ Å	$c = 6.1425$ Å	
	Position	*X*	*Y*	*Z*
Fe(1)	8e	0.219	0.373	0.372
Fe(2)	4c	0.217	0	0.251
Fe(3)	4d	0	0.701	0.725
Fe(4)	4d	0	0.208	0.152
Fe(5)	2b	0	0.5	0.083
Fe(6)	2a	0	0	0.607
P, Si(1)	8e	0.273	0.332	0.976
P, Si(2)	2b	0	0.5	0.517
P, Si(3)	2a	0	0	0.981

The hexagonal phase of Fe_2P, containing nine atoms in the unit cell, may be represented as a BCO structure with 18 atoms (12 Fe and six P) per primitive cell. It turns out that the P(I) type atoms of the hexagonal crystal structure correspond to the P(1) type atoms of the BCO structure, whereas the P(II) type atom correspond to one P(2) type atom and one P(3) type atom in the BCO structure. For the Fe sites, the three Fe(I) type atoms of the hexagonal structure are transformed into four Fe(1) and two Fe(2) type atoms of the BCO structure, whereas the other Fe type, Fe(II), of the hexagonal lattice corresponds to two Fe(3) type, two Fe(4) type, and one each of the Fe(5) and Fe(6) sites. These correspondences, shown in figure 2, are useful to have in mind in the discussions below.

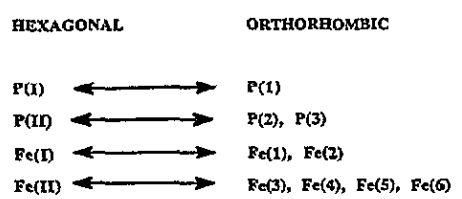

Figure 2. The correspondence between the P and Fe sites of the hexagonal and the orthorhombic crystal structures.

3. Experimental results

An alloy $Fe_2P_{0.75}Si_{0.25}$ was synthesized from high-purity elements by the drop synthesis method in an induction furnace. X-ray powder diffraction photographs were taken in a focusing Hägg–Guinier type camera with Cr $K\alpha_1$ radiation and Si as internal calibration standard (a = 5.431 065 Å). The positions and the intensities of the reflexions were measured with a computer controlled microdensitometer. The unit cell dimensions were refined with a local least-squares program. Structure refinements were performed by using the Rietveld method. The structural parameters are listed in table 1 [10].

We have performed Mössbauer absorption measurements in a 6 T superconducting magnet spectrometer on four different samples $Fe_2P_{1-x}Si_x$ with x = 0.10, 0.16, 0.25, and 0.35 at temperatures ranging from 4 K to 295 K.

The Mössbauer equipment was of conventional constant acceleration type utilizing a double-ended vibrator with ^{57}CoRh sources at both ends. One source was used to simultaneously record calibration spectra, using natural Fe foils at room temperature as reference absorber. A detailed report concerning the preparation, measurement, and analysis of the result has been published elsewhere [11]. Here we only report results essential for this article. It is quite clear that the BCO samples become fully magnetically polarized in a field of 1.5 T with the Fe moments parallel to the external field. Since the γ-ray is parallel to the external field the lines with $\Delta m = 0$ in each sextet disappears, making the analysis of the Mössbauer spectra easier. An example of the spectra and the fitting is given in figure 3.

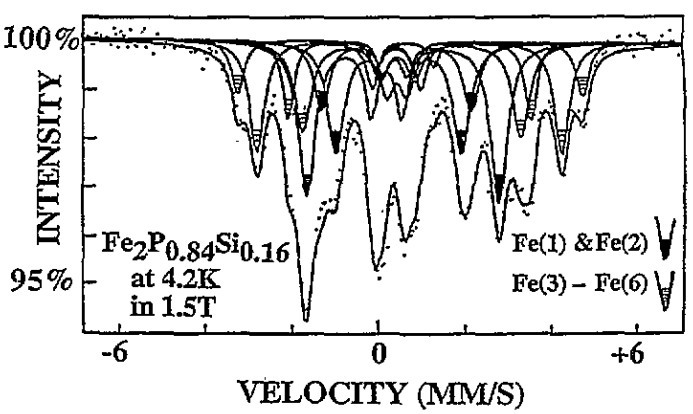

Figure 3. The Mössbauer spectra of $Fe_2P_{0.84}Si_{0.16}$ at 4.2 K and in an external field of 1.5 T. Different Fe site patterns are indicated.

It turned out to be impossible to fit the BCO sample spectra with six different patterns emanating from six different Fe sites. Since Fe in the real sample is surrounded by Si atoms (instead of only P as in our theoretical approach) in varying amounts one can easily imagine that each Fe site could give rise to different six-line patterns. We were however able to obtain good fits by only using seven different patterns, the Fe(1) atoms with a nominal intensity of 33% of total Fe giving two closely lying patterns. The average results for the magnetic hyperfine fields at 4.2 K for $x = 0.16$ and $x = 0.25$ are -14 T, -10 T, -17 T, -23 T, -26 T, and -19 T for Fe(1)–Fe(6) respectively. The value for Fe(1) is an average from the two patterns for Fe(1) mentioned above.

The ascriptions between Mössbauer patterns and the Fe sites have been made partly from intensity and isomer shifts results and partly from results from our electronic structure calculation.

The magnetic hyperfine fields at 15 K for hexagonal Fe have been reported to be -11.4 T for Fe(I) and -18.0 T for Fe(II), as a comparison [12].

4. Calculated electronic structure

We have performed self-consistent scalar relativistic calculations using the linear muffin tin orbital method [13] in the atomic sphere approximation (ASA). The LSDA was used, with the exchange and correlation potential suggested by von Barth and Hedin [14]. The state density was calculated with the tetrahedron method [15]. In subsection 4.1 we present self-consistent calculations for the orthorhombic structure. In subsection 4.2 we discuss theoretically the hyperfine fields from the different Fe sites. In all the calculations presented here, the Fe 3d, 4s and 4p states were treated as valence states. For the P atoms the 3s and 3p states were included in the band structure. Also 3d states on the P atoms are included in the basis set. All other electrons were treated as being part of the core charge density, which was not iterated, but kept frozen equal to the atomic charge density. A fully relativistic atomic program was used to generate this core density.

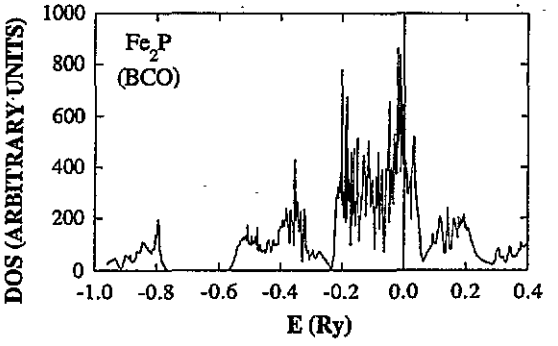

Figure 4. The total paramagnetic DOS for the BCO structure. The Fermi energy is marked by a vertical line.

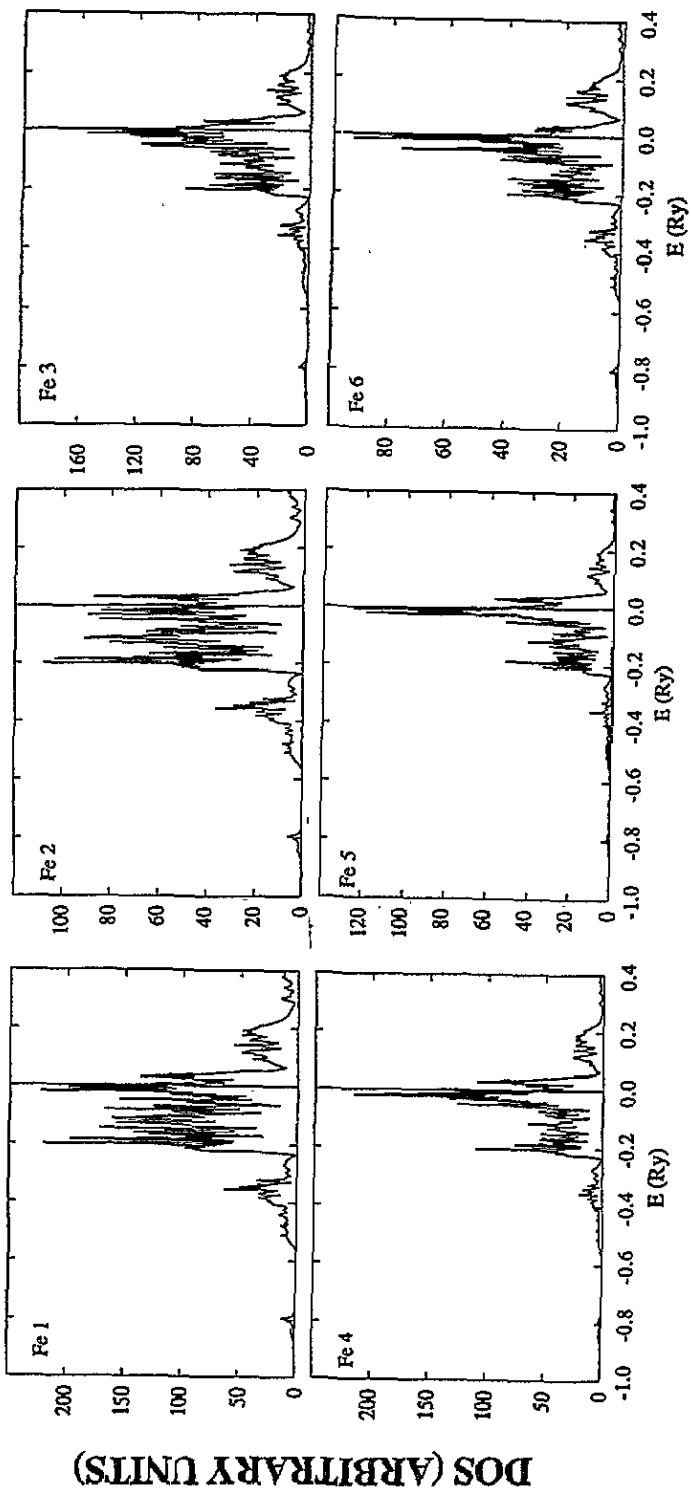

Figure 5. The projection of the paramagnetic DOS for the BCO structure into its Fe(1)–Fe(6) components. The Fermi energy is marked by a vertical line at zero energy.

4.1. Body centred orthorhombic structure

In table 1 the lattice parameters and the atomic positions of the BCO structure are given. These are the input data for our calculations. Experimentally this phase is observed when some of the P atoms are replaced by Si atoms (figure 1). Thus in the Mössbauer data some Fe sites will not have the same symmetry as if these Si substitutions are ignored. We believe, however, that the main effect of the Si substitution is to stabilize the orthorhombic structure, and that this substitution does not change the magnetic properties, as such, significantly. Thus this calculation was done assuming a stoichiometric BCO Fe_2P structure. In section 2 the details of this phase were discussed. In this structure there are three inequivalent P sites and six different Fe sites, and it may be considered as a distortion of the hexagonal structure. In figure 4 the total paramagnetic DOS is presented. It is quite similar to what was obtained in the case of the hexagonal lattice [7]. The main difference (compared to the calculation of the hexagonal compound in [7]) is the peak at approximately −0.8 Ryd, which is due to the fact that we have included the P 3s states in our calculation, whereas these states were considered to be part of the core in [7]. Figure 4 shows that these states are indeed separated from the rest of the band structure by a gap several electronvolts wide, and therefore they hybridize very little with the rest of the band structure. Thus treating them as part of the core is justified *a posteriori*. The main part of the spectrum, however, is dominated by the P 3p states, which are mainly situated between −0.6 Ryd and −0.2 Ryd, and the Fe 3d states at −0.2–0.1 Ryd. These states do hybridize strongly. The state density at E_F (the Fermi energy is put at zero energy in all figures) is quite large and one might therefore conclude that a spin polarized solution will be stable, resulting in moments quite similar to what was obtained in the hexagonal case. However, closer inspection of the site projected paramagnetic DOS reveals large differences between the sites. In figure 5 the hybridization between the 3d states of the Fe(1) and Fe(2) sites and the P 3p states can be seen to be quite large, since there is a substantial 3d character in the energy region between −0.6 and −0.4 Ryd. Also note that the Fe(1) and Fe(2) d bands have approximately the same shape and weight throughout the whole 3d bandwidth (apart from a factor of two, reflecting that there are four Fe(1) sites in the cell, but only two Fe(2) sites). The DOSs of these two Fe sites differ quite substantially in character from the DOS of the Fe(3)–Fe(6) sites, which are also displayed in figure 5. The obvious difference is that the DOS is much more sharply peaked close to the Fermi energy for the Fe(3), Fe(4), and Fe(5) sites. This will of course be reflected in the magnetic properties obtained from a spin polarized calculation. In table 2 some results obtained from this non-polarized calculation are presented. The charge transfer (denoted by 'charge' in table 2) is seen to be quite small. Interestingly the Fe(1) and Fe(2) atoms are the only sites with a small positive charge transfer, i.e. they have more electrons than the eight that correspond to a neutral Fe atom. Interestingly, in the hexagonal structure it is only the Fe(I) site that also has a positive charge transfer. This further substantiates the correspondence between the sites of the two structures shown in figure 2. The P 3p and the Fe 3d occupation numbers are also given in table 2. The P 3p occupations vary between 2.62 for the P(2) site to 2.78 for the P(1) site. The variation in the Fe 3d occupations, though, is much smaller, the d occupation being roughly equal to 6.70, which is close to the 3d occupation in BCC Fe. This only reflects the fact that the 3d states of Fe are more localized than the P 3p states.

The magnetic moments, obtained in a spin polarized calculation, are presented in table 3. The corresponding total spin polarized DOS for the BCO structure is presented in figure 6. The shape of this state density is quite similar to what is obtained for the hexagonal structure. Also, we calculate the total moment to be $2.99\mu_B$ per formula unit, very close to the total spin moment obtained for the hexagonal Fe_2P. Nevertheless, large differences between the

Table 2. Results from the paramagnetic (non-spin-polarized) calculation for the BCO structure. 'Charge' is the charge transfer; N_{3d} and N_{3p} are the 3d and 3p occupations of Fe and P, respectively.

	P(1)	P(2)	P(3)	Fe(1)	Fe(2)	Fe(3)	Fe(4)	Fe(5)	Fe(6)
Charge	−0.11	−0.06	−0.10	+0.15	+0.18	−0.07	−0.04	−0.14	0.00
N_{3d}	—	—	—	6.70	6.70	6.72	6.69	6.73	6.70
N_{3p}	2.78	2.62	2.67	—	—	—	—	—	—

Table 3. Calculated spin moments for the orthorhombic structure. The spin moments are decomposed into its site and angular momentum components.

	μ_s (μ_B)	μ_p (μ_B)	μ_d (μ_B)	μ_{tot} (μ_B)
P(1)	−0.005	−0.083	−0.022	−0.110
P(2)	−0.004	−0.045	−0.047	−0.096
P(3)	−0.007	−0.058	−0.038	−0.103
Fe(1)	−0.008	−0.016	+1.080	+1.056
Fe(2)	−0.008	−0.019	+0.750	+0.723
Fe(3)	+0.008	+0.004	+2.031	+2.043
Fe(4)	+0.009	+0.009	+2.260	+2.278
Fe(5)	+0.011	+0.012	+2.628	+2.651
Fe(6)	+0.009	+0.005	+1.600	+1.614

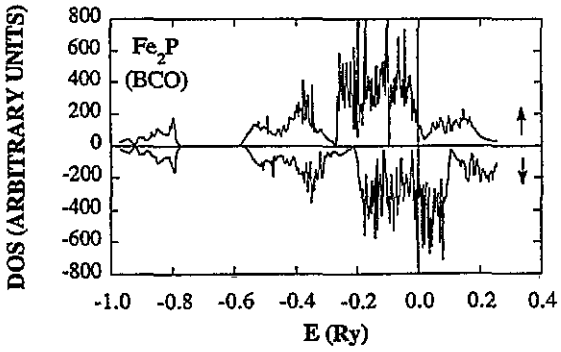

Figure 6. The spin polarized DOS for the BCO structure. The arrows denotes the spin direction and the Fermi energy is marked by a vertical line at zero energy.

Fe sites are revealed from table 3. As expected, also for this compound the moments on the P atoms are quite small; they are of an induced type, i.e. these moments exist only due to the hybridization with the spin split Fe 3d bands and they polarize antiparallel to the Fe moments. Let us now consider the Fe moments. Figure 7 shows that there are only minor differences between the DOSs of the Fe(1) and Fe(2) sites. The difference in weight is due to the factor of two ratio in the number of sites of the two types (just as in figure 5). The calculated spin moments are $1.06\mu_B$ and $0.72\mu_B$ for the Fe(1) and Fe(2) atoms, respectively. The spin moments on these sites are not saturated, since there is a substantial 3d character above the Fermi energy for the majority spin direction. This is in sharp contrast to the Fe(3), Fe(4), and Fe(5) sites. Their spin polarized DOS (together with that of the Fe(6) site) are plotted in figure 7. Their spin moments are clearly quite saturated. This is especially so for the Fe(5) site. Here the spin up DOS is almost completely filled, whereas a large

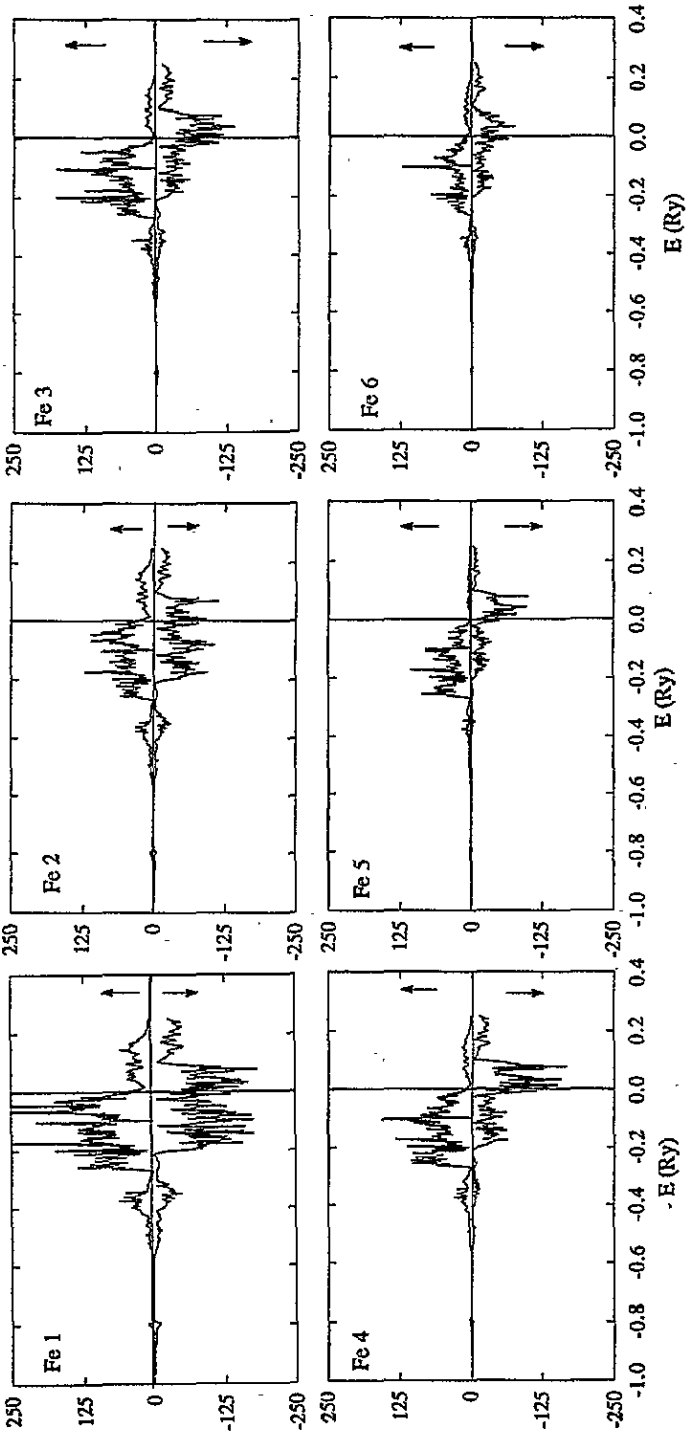

Figure 7. The projection of the spin polarized DOS into its Fe(1)–Fe(6) site components.

part of the spin down spectrum is above E_F. The calculated spin moment on this site is $2.65\mu_B$. This is an extremely large value (in BCC Fe the spin moment is $2.2\mu_B$), and is close to the border of how large an Fe moment may become [16]. Also the Fe(3) and Fe(4) spin moments are quite large, $2.28\mu_B$ and $2.04\mu_B$ respectively. These Fe atoms clearly act as strongly ferromagnetic sites, in the traditional sense. For the Fe(6) site, however, the spin moment is not completely saturated and it is much smaller, only $1.61\mu_B$. For the Fe moments, it is quite interesting to note that the 4s4p conduction band polarizes antiparallel to the 3d band for the Fe(1) and Fe(2) atoms, whereas these moments are parallel for the Fe(3)–Fe(6) atoms. This is quite interesting, since from quite general arguments [17] (see also below) one would expect the 4s conduction band to polarize antiparallel to the narrow 3d band if the latter were more than half filled, but parallel if the 3d band were less than half filled. This is confirmed from spin polarized calculations of the late 3d transition metals, where the 4s4p conduction band polarizes antiparallel to the 3d moment. One would then expect an early transition metal such as V, say, to have a parallel polarization of the conduction band if it were magnetic. Now V is not a ferromagnet, but we have performed a fixed moment calculation where we have forced the system to be magnetic (effectively by applying a magnetic field on the d band). Such a calculation reveals a 4s4p polarization parallel to the 3d moment. Thus the Fe(3), Fe(4), Fe(5), and Fe(6) atoms are anomalous in this respect. The same is true for the Fe(II) site of the hexagonal structure. This is gratifying, since we noted in section 2 that Fe(3)–Fe(6) corresponded to Fe(II) of the hexagonal structure, whereas Fe(1) and Fe(2) of the BCO structure corresponded to the hexagonal Fe(I) site. There are essentially two competing effects that determine the sign of the conduction electron polarization. First the spin split 3d states introduce an asymmetry between the two spin directions in the exchange–correlation potential, and thus the 4s4p conduction electrons will see a deeper potential for a parallel spin alignment, leading to a parallel spin polarization of the conduction band and 3d moments. Second, the hybridization between the 4s4p band and the 3d spin split band gives rise to a substantial weight of the 4s4p band at energies where the 3d band is located. Since the centre of the occupied part of the 4s and 4p band is closer to the centre of the occupied 3d band for majority (up) spin than for minority (down) spin the 4s4p–3d hybridization is larger for majority than for minority spin. This leads to a larger admixture of 4s4p character into the 3d spin up band than the 3d spin down band also *at energies above the Fermi energy*, and hence an antiparallel spin alignment. Therefore these two effects seem to cancel one another to a large degree, leaving only a small conduction electron polarization. The latter effect will dominate for more than half-filled 3d bands *provided there are 3d spin up states that are unfilled.* If the magnet is saturated, however, there are no available 3d majority spin states for the conduction electron band to hybridize into, and this will suppress the importance of the second effect, leading to a parallel spin alignment.

4.2. Hyperfine fields

The hyperfine field can be separated into three different contributions: the Fermi contact term, the magnetic dipolar term, and the orbital momentum term. Even though the anisotropy of Fe_2P is unusually large for a 3d compound, the orbital contribution to the hyperfine field is expected to be small as is the classical dipolar term, and therefore in this work we concentrate on estimating the Fermi contact term. In principle this term should be evaluated as a matrix element with the correct wavefunctions. However, even for the elemental ferromagnets Fe and Ni, a fully relativistic and correct calculation, within the LSDA, does not give agreement with experimental data [18]. This is presumably due to the LSDA itself, since in the case of hyperfine fields one is interested in the wavefunctions

close to the nuclei, a region where the density is rapidly varying and therefore the local approximation is likely to fail. Hence approximations which go beyond standard LSDA, such as self-interaction corrected calculations, would be desirable if a more consistent evaluation of these matrix elements were desired. Since we are only interested in a rough estimate we therefore content ourselves with using a much simpler expression for the hyperfine field. In the non-relativistic limit this quantity is given by the expression

$$B_{\mathrm{hf}} = \frac{8\pi}{3}\frac{eh}{2mc}\sum_i[\rho_i^{\uparrow}(0)-\rho_i^{\downarrow}(0)] = 54\sum_i[|\Psi_i^{\uparrow}(0)|^2-|\Psi_i^{\downarrow}(0)|^2] \qquad (\mathrm{T}a_0^3)$$

where the sum is equal to the electron spin density at the nucleus. Thus each orbital contributes an amount proportional to its spin density at the origin. The core contribution consists of the 1s, 2s, and 3s orbitals. The first two terms are negative. This is so because for these two orbitals the majority spin wavefunctions will be pulled out further from the origin than the minority spin wavefunctions since they feel a stronger 3d potential, which is located further out from the nuclei. For the 3s wavefunction the situation is reversed, since it lies outside the 3d wavefunction. Thus the spin up 3s orbital is pushed in more than the 3s down orbital will be, leading to a positive contribution to the hyperfine field from these orbitals. From the discussion in subsection 4.1 we can expect either sign from the 4s conduction band.

In order to calculate the contribution from the core electrons to this sum it is necessary to allow the core orbitals to relax due to the presence of the spin polarized valence bands. We did not perform such a calculation since the frozen core approximation was used. However, for the core contribution to the Fermi contact term there is ample evidence from previous calculations that it scales with the local magnetic moment on the site. Blügel *et al* [20] found that for a 3d atom embedded in a Ni host the proportionality constant was roughly equal to -10.0 T μ_{B}^{-1} throughout the series, and a more precise value of -10.5 T μ_{B}^{-1} could be deduced from the listed data for the Fe impurity. For the ferromagnetic metals, one can deduce a value of -10.9 T μ_{B}^{-1} for Fe and approximately -11.5 T μ_{B}^{-1} for Co and Ni from the calculations by Ebert *et al* [18]. However, as noted, this procedure results in fields that are quite far from the experimental data for Fe and Ni, while fair agreement was obtained for Co. For the substantially more complicated hexagonal Fe_2P Eriksson *et al* [7] noted that the calculated core contribution (using the much simpler expression given above) was proportional to the total moment for the hexagonal Fe_2P, both at equilibrium volume and at compressed volumes, and that the proportionality factor was roughly -12.6 T μ_{B}^{-1}. The same factor leads to a good account also for BCC Fe, where the more proper relativistic calculation fails. Hence we adopt the value -12.6 T μ_{B}^{-1} in the present discussion. In order to obtain a theoretical estimate of the magnetic hyperfine field in BCO Fe_2P, we therefore argue that the following procedure should be quite accurate. The calculated site projected spin moments, for all six inequivalent Fe sites, are compared with the site projected moments calculated by Eriksson *et al*, and their core contributions to the hyperfine field are appropriately scaled. To this we add the valence band contribution, which stems from the 4s electrons, which we have calculated self-consistently. In figure 8 we present the self-consistently calculated valence contribution to the spin density. Close to the nuclei the 4s polarization dominates over the 3d spin splitting and hence the contribution from the 3d electrons is ignored in our treatment. For the BCO structure the valence electron spin density is plotted for the Fe(1) and Fe(2) sites in the top panel, and for the Fe(3), Fe(4), Fe(5), and Fe(6) atom types in the bottom part of the figure. Also for this structure the spin density behaves as one would expect close to the origin, being negative for the top

panel but positive for the bottom panel of figure 8. Here it is in order to note the drastic increase in the spin density close to the origin for the BCO Fe(3)–Fe(6) sites. This is then a likely source of error when estimating the valence contribution to the hyperfine field. From our calculation there is a small difference between the spin densities close to the nuclei for the Fe(1) and Fe(2) sites. The spin densities of the Fe(3)–Fe(6) sites are close to one another at the nuclei. From our calculations we obtain the values −0.084, −0.088, 0.152, 0.167, 0.205, and 0.155 for the spin density (in a_0^{-3}) at the nuclei for the Fe(1)–Fe(6) sites, respectively. In table 4 we compile the core contributions that we estimate by simply using the scaling factor -12.6 T μ_B^{-1}. B_v denotes our calculated valence contribution and finally B_{hf} is the sum of these and thus our theoretical estimate of the hyperfine field in BCO Fe_2P. Comparing with the experimental data, which are also given in table 4, fair or good agreement is obtained for all sites but the Fe(6) site. Eriksson and Svane [19] performed a rather extended investigation of the hyperfine fields in a number of compounds. They found that for those compounds they investigated that had an unsaturated spin up band, the *total* hyperfine field scaled very well with the local moment, the proportionality factor being -14.2 T μ_B^{-1}. If we adopt this value and multiply with the calculated local moments we obtain fields (−15.1 T for the Fe(1) site and −10.2 T for the Fe(2) site) in very good agreement with those for the unsaturated Fe sites. Eriksson and Svane noted that this procedure failed for the Fe(II) site in the hexagonal compound, as well as for FeO. In these compounds the spin up band was saturated, and also the 4s contribution to the hyperfine field was oppositely directed to the core contribution. Also it is worth noting that the calculated hyperfine fields in the hexagonal parent compound were in better agreement with experiment for the Fe(I) site than for the Fe(II) site [7]. This seems to be generally true also for the BCO structure, even though the agreement for the Fe(3) site is perfect. It should be more difficult to estimate the spin density for the Fe(3)–Fe(6) sites since the spin density varies rather fast close to the nuclei here. If one considers the fact that the spin density decreases very fast away from the nuclei, the positive valence electron contribution for Fe(3)–Fe(6) would be less positive, leading to an increased (negative) hyperfine field for these atoms. Actually a relativistic derivation [20] of the Fermi contact term shows that the spin density at the origin should be replaced by the spin density averaged over a distance from the nuclei equal to the Thomas length Ze^2/mc^2. This means that the hyperfine field is a somewhat more delocalized quantity than for example the isomer shift is, the latter being proportional to the contact density.

Table 4. Theoretical estimates of the Fermi contact term contribution to the hyperfine field for the different Fe sites of the BCO structure. The core contribution, B_c, was estimated by scaling the calculated results for the hexagonal structure as obtained in [7]. The valence contribution, B_v, was calculated self-consistently. All magnetic hyperfine fields are given in tesla. Also given are the calculated magnetic moments in μ_B and the experimental values of B_{hf} found in the Mössbauer study.

	Fe(1)	Fe(2)	Fe(3)	Fe(4)	Fe(5)	Fe(6)
$\mu^{(\text{calculated})}$	1.06	0.72	2.04	2.28	2.65	1.61
B_c (T)	−13.3	−9.1	−25.7	−28.7	−33.4	−20.3
B_v (T)	−4.5	−4.7	+8.2	+9.0	+11.1	+8.4
B_{hf} (T)	−17.8	−13.8	−17.5	−19.7	−22.3	−11.9
B_{hf}^{exp} (T)	−14.4	−10.4	−17.3	−23.0	−26.0	−19.0

The connection between the interatomic distances and the magnetic moments is interesting and will now be commented upon. Fe(I) (or BCO Fe(1) and Fe(2) is surrounded

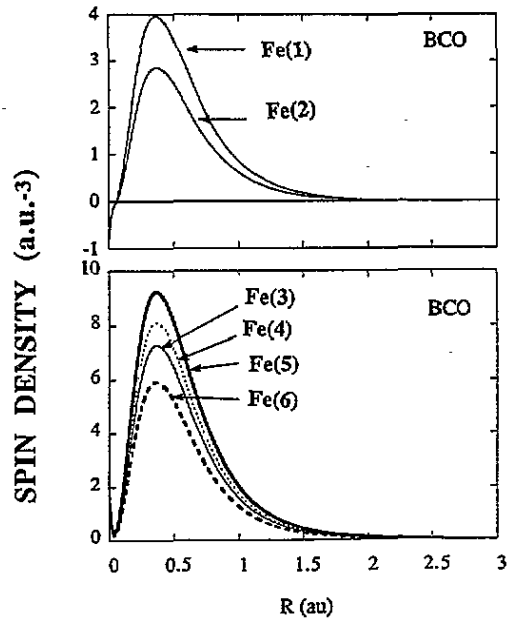

Figure 8. The calculated total valence spin density for the Fe(I) and Fe(2) sites in the BCO structure (top) and the Fe(3), Fe(4), Fe(5), and Fe(6) sites in the BCO structure (bottom). The spin density has been multiplied by 4π.

by four P atoms in a tetrahedral configuration with a distance of ~ 2.2 Å and eight to nine Fe atoms with a distance of ~ 2.7 Å, while Fe(II) (or BCO Fe(3)–Fe(6)) is surrounded by five P atoms in a pyramidal configuration with a distance of ~ 2.5 Å and 10–12 Fe atoms with a distance of ~ 2.9 Å.

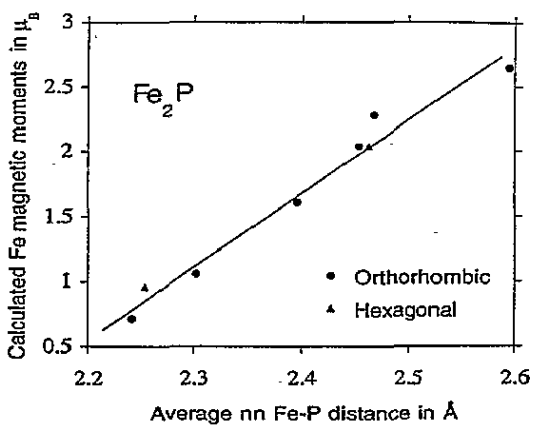

Figure 9. A plot of the Fe moments as a function of the average nearest-neighbour Fe–P distance for the hexagonal and the BCO structure.

The magnetic moments at the pyramidal Fe were found to be larger than the moment for the tetrahedral Fe. In figure 9 we present a plot of the Fe moment versus the average

nearest-neighbour (NN) Fe–P distances. As can be seen the trend mentioned above also holds true when taking the individual moments into account. So it seems that larger Fe–P NN distances are strongly correlated with the polarization of the Fe electrons. Ligands closer to the Fe atoms cause stronger P 3p–Fe 3d hybridization, which decreases the Fe 3d moment.

5. Summary

We have calculated the magnetic moments for the hexagonal and BCO phases of Fe_2P. Hyperfine fields have been measured and calculated. Considering the extreme complexity of the compound, with six inequivalent Fe sites, the calculated values for the hyperfine fields compare very well with the experimental data. It is found that the spin moments vary substantially between different sites (from $0.7\mu_B$ to $2.6\mu_B$) and that there is no simple scaling between the hyperfine fields and the spin moments. This is so because the valence band (4s) contribution to the Fermi contact term may be large and have either sign. Indeed, comparing the Fe(2) and Fe(5) sites (say), the calculated spin moment ratio is 3.68, but the calculated hyperfine field ratio is 1.62.

Acknowledgment

The Swedish Natural Science Research Council is acknowledged for financial support.

References

[1] Beckman O and Lundgren L 1991 *Handbook of Magnetic Materials* vol 6, ed K H J Buschow (Amsterdam: North-Holland) p 181
[2] Jernberg P, Yousif A A, Häggström L and Andersson Y 1984 *J. Solid State Chem.* **53** 313
[3] Bean C P and Rodbell D S 1962 *Phys. Rev.* **126** 104
[4] Wohlfarth E P 1979 *J. Appl. Phys.* **50** 7542
[5] Moriya T and Usami K 1977 *Solid State Commun.* **23** 935
[6] Beckman O, Lundgren L, Nordblad P, Svedlindh P, Törne A, Andersson Y and Rundquist S 1982 *Phys. Scr.* **25** 679
[7] Eriksson O, Sjöström J, Johansson B, Häggström L and Skriver H L 1988 *J. Magn. Magn. Mater.* **74** 347
[8] Ishida S, Asano S and Ishida J 1987 *J. Phys. F: Met. Phys.* **17** 475
[9] Malozemoff A P, Williams A R and Moruzzi V L 1984 *Phys. Rev.* B **29** 1620
[10] Andersson Y *et al* unpublished
[11] Häggström L, Severin L and Andersson Y 1994 *Hyperfine Interact.* at press
[12] Wäppling R, Häggström L, Ericsson T, Devanarayanan S, Karlsson E, Carlsson B and Rundqvist S 1975 *J. Solid State Chem.* **13** 258
[13] Andersen O K 1975 *Phys. Rev.* B **12** 3060
Skriver H L 1984 *The LMTO Method* (Berlin: Springer)
[14] von Barth U and Hedin L 1972 *J. Phys. C: Solid State Phys.* **5** 1629
[15] Jepsen O and Andersen O K 1971 *Solid State Commun.* **9** 1963
[16] In the strongest permanent magnet known, $Nd_2Fe_{14}B$, the largest calculated spin moment is $2.9\mu_B$ for one of the sites. See L. Nordström 1991 *Thesis* Uppsala University
[17] Severin L, Brooks M S S and Johansson B 1994 unpublished
[18] Ebert H 1989 *J. Phys.: Condens. Matter* **1** 9111
Ebert H, Strange P and Gyorffy B L 1988 *J. Phys. F: Met. Phys.* **18** L135
[19] Eriksson O and Svane A 1989 *J. Phys.: Condens. Matter* **1** 1589
[20] Blügel S, Akai H, Zeller R and Dederichs P H 1987 *Phys. Rev.* B **35** 3271